Why Do Grains Remain Roughly Equiaxed during Steady State Discontinuous Dynamic Recrystallization?

Frank Montheillet, David Piot

Why Do Grains Remain Roughly Equiaxed During Steady State Discontinuous Dynamic Recrystallization?

Frank Montheillet[1,a*] and David Piot[2,b]

[1,2]Mines Saint-Etienne, Univ Lyon, CNRS, UMR 5307 LGF,

158 cours Fauriel, 42023 Saint-Etienne, France

[a]montheil@emse.fr, [b]david.piot@mines-stetienne.fr

*emeritus

Keywords: Dynamic recrystallization, grain size, grain boundary migration, grain shape, advection, modeling

Abstract. The combination of advection and migration of grain boundaries is analyzed on the basis of a simple mesoscale model, where parallelepipedic grains are considered under uniaxial compression straining. Strain hardening and dynamic recovery are described by the classical Yoshie-Laasraoui-Jonas equation. Grain-boundary migration is driven by the difference in dislocation densities between one representative grain and the average over the material. Finally, nucleation is assumed to occur at grain boundaries. Special attention is paid to the aspect ratio, which starts from unity (infinitely small cubic nucleus) and tends to zero when the grain disappears. In spite of the role of migration, the average shape of the grains is determined as a first approximation by their lifetimes.

Introduction

Microstructures induced by thermomechanical treatments are of primary importance, because they determine the mechanical properties of the products. The major features are the grain size and the crystallographic texture, but grain shapes are also taken into consideration since equiaxed microstructures are generally desired. In low to medium stacking fault energy materials such as the austenitic stainless steels, such microstructures are precisely obtained by the occurrence of discontinuous dynamic recrystallization (DDRX): When strain is sufficiently large, a steady state is achieved where the average aspect ratio of the grains remains close to one. This is rather unexpected because the *advection movement* of grain boundaries, which follow the material flow, tends to flatten or elongate grains during deformation.

A simple grain scale (or mean field) model has been formerly developed by the authors [1] to analyze various aspects of DDRX steady state, such as the influence of the specific strain hardening and dynamic recovery behaviour of the material [2] or the effect of grain boundary migration induced softening (BMIS) [3]. On the other hand, the combined effects of interphase-boundary advection and migration on the shape change of a second phase particle during growth or dissolution has been recently investigated [4]. However, DDRX grain scale models have so far systematically considered spherical grains, which precludes any change of their aspect ratio. In the present investigation, a new approach involving parallelepipedic grains and including advection is proposed, which leads to simple calculations, while allowing to analyze the evolution of the shape of the grains during DDRX steady state.

Outline of the Model and Mathematical Developments

A set of parallelepipedic grains submitted to uniaxial compression is considered. If the DDRX nuclei are assumed cubic, the grains will keep a quadratic shape during deformation. Let a and b be the current half lengths of the edges of one grain parallel and perpendicular to the compression axis, respectively.

The evolutions of a and b with strain are given by the following two equations:

$$\begin{cases} \dfrac{\mathrm{d}a}{\mathrm{d}\varepsilon} = -a + \dfrac{M\tau}{\dot{\varepsilon}}(\bar{\rho} - \rho) \\ \dfrac{\mathrm{d}b}{\mathrm{d}\varepsilon} = \dfrac{b}{2} + \dfrac{M\tau}{\dot{\varepsilon}}(\bar{\rho} - \rho) \end{cases} . \tag{1}$$

The first terms of the right hand sides are associated with advection (uniaxial compression field), while the second terms correspond to grain boundary migration driven by the difference between the average dislocation density $\bar{\rho}$ of the material and the current dislocation density ρ of the grain. M is the grain boundary mobility, τ is the line energy of the dislocations and $\dot{\varepsilon}$ the prescribed strain rate. The strain dependence of ρ is determined by both strain hardening and dynamic recovery. A modified Yoshie-Laasraoui-Jonas (YLJ) equation will be used here [5]:

$$\frac{\mathrm{d}\rho}{\mathrm{d}\varepsilon} = h - r\rho - \frac{\rho}{V}\frac{\mathrm{d}V}{\mathrm{d}\varepsilon}, \tag{2}$$

where h and r are the strain hardening and dynamic recovery parameters, and V the volume of the grain. The last term on the right reflects the effect of BMIS [3]. Expressing $V = 8ab^2$ and using Eqs (1), the above equation becomes:

$$\frac{\mathrm{d}\rho}{\mathrm{d}\varepsilon} = h - r\rho + \frac{M\tau}{\dot{\varepsilon}}\rho(\bar{\rho} - \rho)\left(\frac{1}{a} + \frac{2}{b}\right). \tag{3}$$

It is convenient at this stage to introduce non-dimensional variables: let $\hat{\rho} = \rho / h$ and $\xi = \bar{\rho} / h$. Equations (1) and (3) can then be rewritten in the form:

$$\begin{cases} \dfrac{\mathrm{d}\hat{a}}{\mathrm{d}\varepsilon} = -\hat{a} + \xi - \hat{\rho} \\ \dfrac{\mathrm{d}\hat{b}}{\mathrm{d}\varepsilon} = \dfrac{\hat{b}}{2} + \xi - \hat{\rho} \end{cases} , \tag{1'}$$

$$\frac{\mathrm{d}\hat{\rho}}{\mathrm{d}\varepsilon} = 1 - r\hat{\rho} - \hat{\rho}(\xi - \hat{\rho})\left(\frac{1}{\hat{a}} + \frac{2}{\hat{b}}\right). \tag{3'}$$

where $\hat{a} = a / L$, $\hat{b} = b / L$, with $L = M\tau h / \dot{\varepsilon}$. The system of the above three equations can be numerically integrated for any given $\hat{\rho}$ to get the strain dependence of the two edges of the grain as well as its dislocation density between its nucleation at $\varepsilon = 0$ ($\hat{a} = \hat{b} = 0$, $\hat{\rho} = 0$) and its disappearance at $\varepsilon = \omega$. More specifically, ω is defined as the strain where the *volume* of the grain goes to zero. Calculations show that the side a parallel to the compression axis always cancels first as expected, which means that the grain vanishes in the form of a flattened pancake.

In order to determine $\hat{\rho}$, a "closure equation" is used, which means that upon steady state each grain gives birth to one unique new grain in its lifetime. This condition can be written in the form [1, 3]:

$$\frac{k_N \bar{\rho}^3}{\dot{\varepsilon}} \int_0^{\omega} \frac{S}{2} \mathrm{d}\varepsilon = 1, \tag{4}$$

where $S = 8b^2 + 16ab$ denotes the surface of the grain, which means that DDRX nucleation occurs mainly at grain boundaries, and the factor $1/2$ accounts for the fact that each boundary is shared by two grains. k_N is a nucleation parameter which characterizes the nucleation rate.

Introducing the non-dimensional variables into (4) leads to:

$$\frac{4k_N M^2 \tau^2 h^5}{\dot{\varepsilon}^3} \xi^3 G(\xi, r) = 1, \tag{5}$$

which can be inverted to give:

$$\xi^3 G(\xi, r) = \frac{\dot{\varepsilon}^3}{4k_N M^2 \tau^2 h^5} = A, \tag{5'}$$

where the integral $G(\xi, r) = \int_0^{\omega} (\hat{b}^2 + 2\hat{a}\hat{b})\, \mathrm{d}\varepsilon$ has no analytical expression in the general case.

It is important to note that, except for *r*, all material parameters (usually strain rate and temperature dependent) and deformation conditions are collected in the variable *A*, while the left hand side of Eq. (5') depends only on ξ and *r*.

In Fig. 1, ξ is plotted as a function of $A = \xi^3 G(\xi, r)$ for various values of the dynamic recovery parameter *r*. In the absence of dynamic recovery ($r = 0$), the double logarithmic curve is perfectly approximated by a straight line, which means that ξ is a power law function of *A*, *viz.*:

$$\xi = 0.710\, A^{0.124}. \tag{6}$$

This is no longer the case when *r* is not zero, although the above approximation is still valid for values of *A* less than roughly 10^{-9}. In any case, the average dislocation density $\bar{\rho}$ of the material can be determined with the help of Eq. (5'), as soon as the material parameters are known. It should be noted that $\bar{\rho} < \rho_\infty = h/r$, where ρ_∞ is the virtual steady state dislocation density *in the absence of DDRX*, wherefrom $\xi < 1/r$.

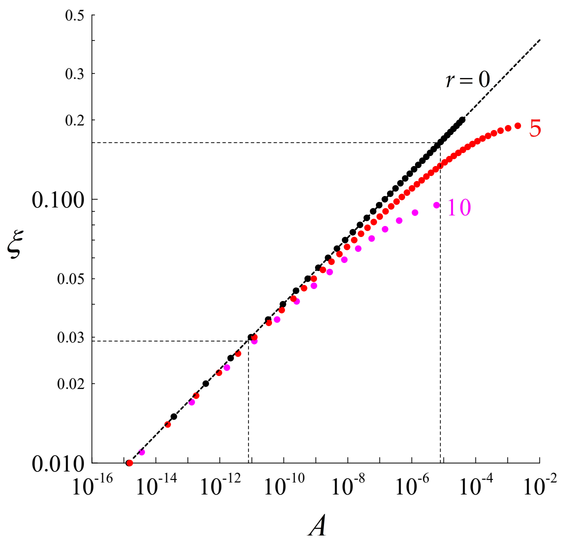

Figure 1. ξ *vs.* *A* double logarithmic plot for various values of the strain rate sensitivity parameter *r*

Results and Conclusions

A first set of results is reported below, for which material parameters pertaining to a high purity Ni-1 %Nb alloy, deformed at a temperature of 900 °C, and strain rates of 10^{-2} and $1\,\mathrm{s}^{-1}$ were used [3]: $k_N = 5\mathrm{x}10^{-9}$ $\mu\mathrm{m}^4\mathrm{s}^{-1}$, $M\tau = 0.1\,\mu\mathrm{m}^3\mathrm{s}^{-1}$, and $h = 1000\,\mu\mathrm{m}^{-2}$. It has been observed that the strain-hardening exponent *h* does not vary significantly with strain rate [6]. On the other hand, the possible strain-rate dependences of k_N and $M\tau$ are not established to date. We will therefore assign the same values to the three parameters for the two strain rates. The main data and model predictions are reported in Table 1.

Table 1. Material data used in the model and some selected predictions

$\dot{\varepsilon}\,[\mathrm{s}^{-1}]$	A	ξ	ω	t_ω[s]	$\overline{v}_m[\mu\mathrm{m.s}^{-1}]$	$\overline{\lambda}(S_z)$	$\overline{\lambda}_0(S_z)$
0.01	$7.854\mathrm{x}10^{-12}$	0.029	0.121	12.1	1.396	0.930	0.915
1	$7.854\mathrm{x}10^{-6}$	0.164	0.639	0.639	7.695	0.699	0.659

Figures 2a and b show the evolutions of the two semi-axes of the grains during their lifetimes at the two strain rates $\dot{\varepsilon} = 0.01$ and $1\,\mathrm{s}^{-1}$. The broken line represents the dislocation density and the critical value $\rho = \overline{\rho}$ is indicated, which corresponds to the strain where the volume $V = 8ab^2$ of the grain goes through its maximum. The diagram shows that the maximum values of *a* and *b* are slightly shifted backward and forward, respectively. Comparison of the two diagrams shows that the "grain size" (estimated for instance by the average of the two axes) is lower at the larger strain rate, whereas the strain when the grain disappears ($\varepsilon = \omega$) is much larger (Fig. 2b). Its dislocation density is then five time larger than at $0.01\,\mathrm{s}^{-1}$. This means that increasing the strain rate slows down DDRX, as expected.

More specifically, the current migration rate of the boundaries is given by $v_m = M\tau\left|\overline{\rho} - \rho\right|$, where the absolute value reflects the fact that $v_m > 0$. The *average* migration rate weighted by the surface of the grain $S = 8b^2 + 16ab$ is then:

$$\overline{v}_m = M\tau \int_0^\omega \left|\overline{\rho} - \rho\right| S\, d\varepsilon \Big/ \int_0^\omega S\, d\varepsilon\,. \tag{7}$$

This gives $\overline{v}_m = 1.396$ and 7.695 $\mu\mathrm{m\,s}^{-1}$ at 0.01 and $1\,\mathrm{s}^{-1}$, respectively. At the same time, the lifetime of the grain $t_\omega = \omega / \dot{\varepsilon}$ drops from 12.1 to 0.164 s, which opposes the increase of the migration rate.

Figures 2c and d were obtained from a former version of the model: they display the evolutions of *spherical grains* deformed in the same conditions without advection effects. Comparison with Figs 2a and b shows that the grain sizes, lifetimes and dislocation densities are not significantly modified by advection.

It is not possible to assess directly the effect of grain boundary migration, since in the absence of the latter no nucleation and therefore no DRX can take place. Nevertheless the main contribution of the present model is to allow the evaluation of the *shape changes* of the grains, which is quantified by the aspect ratio $\lambda = a/b$. In Fig. 3, S_z is one quarter of the current section of the grain parallel to the compression axis, *i.e.* $S_z = a\,b$, which is commonly observed and measured in metallography. The aspect ratio is plotted along the horizontal axis. In other words, the diagrams exhibit distribution functions of the aspect ratios of the grains weighted by their section areas. Upon nucleation, $\lambda = 1$ by assumption and it then decreases continuously as a result of advection until it reaches zero when the grain disappears. Note that the aspect ratio decreases with increasing strain, as expected in compression. The curves are displayed for three values of the recovery parameter, *viz.* $r = 0$, 2.5 and 5 at $0.01\,\mathrm{s}^{-1}$ (Fig. 3a) and $r = 0, 1$ and 2 at $1\,\mathrm{s}^{-1}$ (Fig. 3b), respectively. The horizontal broken line indicates half the maximum of S_z for $r = 0$.

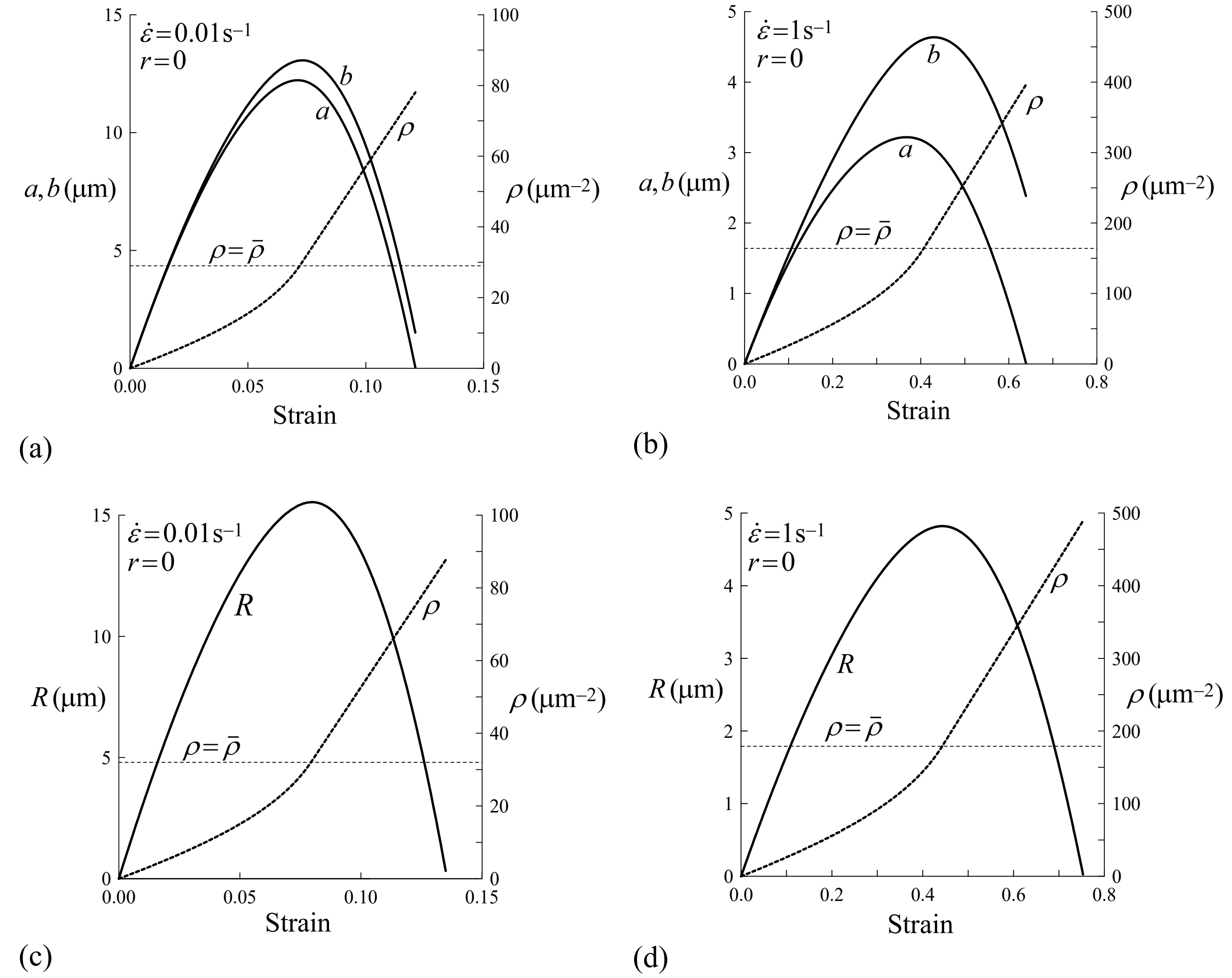

Figure 2. Evolutions of the semi-axes and the dislocation densities of the grains during their lifetimes at (a) $\dot{\varepsilon} = 0.01$ and (b) $1\,\mathrm{s}^{-1}$; (c) and (d): evolutions of spherical grains without advection

At $\dot{\varepsilon} = 0.01\,\mathrm{s}^{-1}$, all grains with a significant size have a large aspect ratio. More quantitatively, for all grains of section area larger than half the maximum, $\lambda > 0.85$, which means that they are almost equiaxed. By contrast, at $\dot{\varepsilon} = 1\,\mathrm{s}^{-1}$, the area fraction of flattened grains is much larger and for the population of larger grains, $0.45 < \lambda < 0.85$. The weighted averages by S_z, referred to as $\overline{\lambda}(S_z)$ are given in Table 1. A tentative comparison is proposed with the case of an initially spherical grain of *finite radius* (in contrast with a DDRX nucleus) submitted to the same compression strain of amplitude ω in the absence of grain boundary migration. The weighted average aspect ratio can be derived analytically:

$$\bar{\lambda}_0(S_z) = \frac{1}{4}\frac{1-\exp(-2\omega)}{1-\exp(-\omega/2)} \tag{8}$$

and numerical values are reported in Table 1. They are only slightly lower than in the previous two cases. Although this comparison is questionable, it suggests the conclusion that the effect of migration is limited during DDRX and therefore that the shape of the grains is mainly determined by their lifetimes.

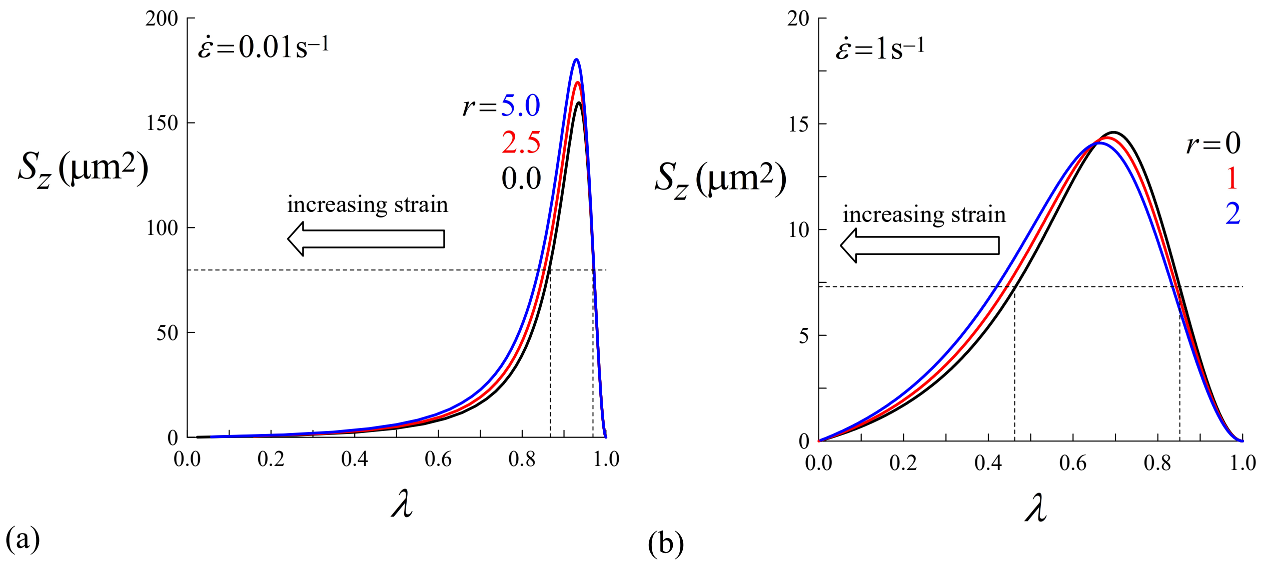

Figure 3. Distribution functions of the aspect ratios of the grains weighted by their section areas at (a) $\dot{\varepsilon} = 0.01$ and (b) $1\,\mathrm{s}^{-1}$

References

[1] F. Montheillet, J.J. Jonas, Models of recrystallization, in: D.U. Furrer, S.L. Semiatin (Eds.), Fundamentals of Modeling for Metal Processing, ASM Handbook, vol. 22A, ASM International, Materials Park, Ohio, 2009, pp. 220-231.

[2] F. Montheillet, D. Piot, Influence of strain hardening and dynamic recovery on DDRX steady state, Thermec-2021, Online Conference, in: M. Ionescu, Ch. Sommitsch, C. Poletti, E. Kozeschnik, T. Chandra (Eds.), Materials Science Forum, 1016 (2021) 194-199.

[3] F. Montheillet, Influence of boundary migration induced softening on the steady state of discontinuous dynamic recrystallization, Materials, Special Issue ″Dynamic Recrystallization Behaviors in Metals and Alloys″ 14 (2021), 3531.

[4] F. Montheillet, A. Aoufi, D. Piot, Combined effects of interphase-boundary advection and migration during particle growth or dissolution, Comp. Mater. Sci. 209 (2022) 111357.

[5] A. Laasraoui, J.J. Jonas, Prediction of steel flow stresses at high temperatures and strain rates, Metall. Trans. A 22 (1991) 1545-1558.

[6] N. Maatougui, D. Piot, M.L. Fares, F. Montheillet, S.L. Semiatin, Influence of niobium solutes on the mechanical behaviour of nickel during hot working, Mater. Sci. Eng. A 586 (2013) 350-357.